Progress In Electromagnetics Research C, Vol. 112, 99–111, 2021

Stubs and Slits Loaded Partial Ground Plane Inspired Hexagonal Ring-Shaped Fractal Antenna for Multiband Wireless Applications: Design and Measurement

Narinder Sharma[1, *] and Sumeet S. Bhatia[2]

Abstract—A multiband hexagonal ring-shaped fractal antenna with stubs and slits loaded partial ground plane has been presented in this manuscript. The proposed antenna is compact in size $24 \times 30 \times 1.6\,\text{mm}^3$ and exhibits enhanced bandwidth, gain, and reflection coefficient. Measured results exhibit that the proposed antenna resonates with impedance bandwidth ($S_{11} \leq -10\,\text{dB}$) in the frequency ranges 1.0–2.75 GHz, 4.74–8.70 GHz, 11.04–12.76 GHz, 14.97–16.62 GHz, and 19.70–22.0 GHz. These frequency ranges cover distinct wireless standards such as 1800 MHz 2G spectrum of GSM band (1.71–1.88 GHz), LTE 2300/LTE 2500 (2.3–2.4 GHz/2.5–2.69 GHz), RFID/Bluetooth (2.4 GHz), 5G spectrum band (5900–6400 MHz) adopted by European Union, Long Term Evolution (LTE) band 46 (5150–5925 MHz), RFID (5.4 GHz), WLAN (5.15–5.35 and 5.72–5.85 GHz), Wi-MAX (5.25–5.85 GHz), FSS (11.45–11.7/12.5–12.75 GHz), defence systems (14.62–15.23 GHz), aeronautical radio navigations (15.43–17.3 GHz), and fixed/mobile satellite communications (19.7–20.1 GHz and 20.2–21.2 GHz). The proposed antenna reveals the positive value of peak realized gain with almost omnidirectional radiation patterns in E- and H-planes for all the resonant frequency bands. The performance of proposed antenna has been realized by using HFSS V13 simulator based on FEM (Finite Element Method), and the results are compared with the experimental results which are in good agreement with each other.

1. INTRODUCTION

In the erstwhile era, paramount changes have been made by the renowned researchers in the field of wireless technology. Wireless communication is a vital part of wireless technology which is insignificant without scrupulous antenna designing. Antenna can be referred as the soul of the wireless communication. Versatile, compact sized, economical, and proficient to perform multiple tasks antennas are in huge demand. The word fractal was firstly introduced by B. Mandelbort in the year 1970 [1]. Fractal means broken into parts, and its examples are available in the nature such as snowflakes, pea cock fins, and broccoli. Therefore, fractals can be derived by using various methods, techniques, etc. Iterative Function System (IFS) is one of the most powerful tools used to create fractals. Commonly used fractal shapes for designing the antennas are Koch, Minkowski, Sierpinski Carpet/Gasket, Hilbert, Meander, Moore, etc. [2]. Though fractal antenna is efficient to exhibit afore-said qualities, the composition of these fractal geometries may create wonders in terms of enhancement of performance parameters. By considering this, many of the researchers have led to this direction and amalgamated the distinct or same type of fractal geometries together to design a new antenna named as Hybrid Fractal Antenna (HFA). Sharma and Bhatia [3] have demonstrated Double Split Labyrinth Resonator (DSLR) based CPW-fed Hybrid fractal antennas (overall dimensions: $30 \times 30 \times 1.6\,\text{mm}^3$) which have

Received 6 April 2021, Accepted 22 April 2021, Scheduled 26 April 2021

* Corresponding author: Narinder Sharma (dr.narinder.sharma0209@gmail.com).

[1] Department of Electronics and Communication Engineering, Amritsar College of Engineering and Technology, Amritsar, Punjab 143001, India. [2] Electronics and Communication Engineering Department, Yadavindra College of Engineering and Technology, Guru Kashi Campus, Punjabi University, Talwandi Sabo, Bathinda, Punjab, India.

been designed by combining the Hilbert and Koch fractal geometries named as Hilbert Koch-Koch Hybrid Fractal Antenna (HKKHFA) and differ from each other in terms of feed line position only. The proposed HKKHFA with Left and Right CPW-feed have also been loaded with DSLR on the reverse side of the substrate for obtaining wideband characteristics (Maximum bandwidth −7.69/7.36 GHz), better impedance matching, and enhanced gain (4.40/4.95 dB). Sharma et al. [4] have presented a $45 \times 38.92 \times 1.6\,\text{mm}^3$ volumetric dimensions HFA designed by the coalescence of Sierpinski Carpet and Minkowski. The proposed HFA has operated on five distinct unique frequencies, i.e., 3.43 GHz, 4.78 GHz, 6.32 GHz, 8.34 GHz, and 9.64 GHz, and is suitable for various wireless applications such as Wi-Max, C-band applications, point-to-point High speed wireless communication, and X-band applications. Sharma and Sharma [5] have exemplified a Microstrip Patch Antenna (MPA) using two different hybrid fractal slots created by uniting Koch-Minkowski and Koch-Koch fractal geometries. Partial Ground Plane length has been varied to attain the optimal length and reported as 8 mm. The MPA with Koch-Minkowski slot has projected bandwidth (2260 MHz), gain (6.1 dB) at resonance points 2.47 GHz and 8.92 GHz, whereas HFA with Koch-Koch slot has discerned bandwidth (2440 GHz), gain (5.62 dB) at operative frequencies 2.77 GHz and 8.62 GHz. Kaur and Sivia [6] have portrayed an antenna (MKGA) designed by concatenation of three fractal geometries like Minkowski, Giuseppe Peano, and Koch curves, and the experimental results of MKGA have exhibited reflection coefficients −18.23 dB and −12.71 dB at respective resonance points 2.44 GHz and 5.84 GHz, along with excellent gains of 4.69 dB and 15.11 dB which made MKGA suitable for Scientific and Medical (ISM) frequency bands. Bangi and Sivia [7] have depicted an HFA (dimensions: $41.5 \times 37\,\text{mm}^2$) which has been created by fusing three distinct fractal geometries as Koch, Minkowski, and Moore. The proposed HFA has been investigated for various parameters such as reflection coefficients, VSWR, radiation pattern, and gain, and even defected ground plane was introduced for improving the performance of HFA. Kumar and Sing [8] have elaborated an HFA designed by fusing two distinct fractal Koch and Minkowski geometries. The HFA reported in this manuscript has adorned seven different operation bands along with permissible limits of performance parameters such as reflection coefficient, VSWR, and gain which made it useful for various mobile wireless applications. Shahu et al. [9] have proposed a UWB bandpass filter (BPF) designed by combining Minkowski and Koch fractal geometries. A Defected Ground Structure (DGS) has also been introduced for enhancing the performance. The designed BPF has revealed a permissible range of return-loss bandwidth, insertion loss, and very wide upper-stopband (11.4 GHz to 20 GHz). Choukiker et al. [10] have projected an HFA designed by the amalgamation of Minkowski Island and Koch geometries. T-shaped strip and rectangular slot have also been introduced for getting the enhanced performance parameters. The various antenna parameters such as peak realized gain, radiation pattern, and scattering parameters have been analyzed at distinct frequencies and in acceptable limits which made it a suitable candidate for handheld mobile devices. A triple band HFA has been revealed by Sharma et al. in [11], and the proposed HFA has been developed by mixing Koch and Minkowski fractal geometries together. The performance parameters of the HFA have been investigated and found in acceptable limits which made this antenna useful for WLAN and RFID applications. Bangi and Sivia [12] have proposed two HFAs by integrating Koch and Minkowski geometries and entitled as Koch-Minkowski Hybrid Fractal Antenna (KMHFA) and Minkowski-Koch Hybrid Fractal Antenna MKHFA. Both the antennas have exhibited performance parameters like VSWR, radiation pattern, and gain in adequate limits in which these antennas are useful for wireless applications. Goyal et al. [13] have developed a dual-band HFA by concatenating Koch and Minkowski geometries together. The proposed HFA has presented bandwidths of 1.05 GHz and 570 MHz at resonance points 4 GHz and 7 GHz. The performance parameters such as reflection coefficient, VSWR, and radiation pattern of the HFA have been in acceptable limits, due to which it became suitable for C and X band applications. Kaur et al. [14] have designed a hexagonal ring-shaped antenna based on staircase fractal geometry for dual-band wireless applications at 4.5 and 7.3 GHz. Similarly, a hexagonal ring fractal antenna has been designed by Mark et al. [15] for multiband wireless applications. In this design, the authors have used a dumbbell-shaped defected ground structure to enhance the performance parameters of designed antenna. Sharma and Bhatia [16] have also designed a nested hexagonal ring-shaped radiating patch for the enhancement of performance parameters for multiband integrated wideband wireless applications. Rathod et al. [17] have demonstrated a low-profile antenna based on a hexagonal ring-shaped patch for biomedical application at 2.4 GHz ISM band. A microstrip hexagonal ring antenna has been investigated

by Ray et al. [18], and the proposed antenna exhibited the resonant frequency band at 2.035 GHz with the corresponding gain of 8.4 dB. Likewise, a hexagonal ring-shaped split ring resonator was introduced in the hexagonal ring-shaped patch by Daniel and Selvaraj [19], and the designed antenna resonated at 5.8 GHz with an impedance bandwidth of 1180 MHz.

By meticulously studying the above-said literature, the authors are motivated from the shapes of antenna discussed in [14–19], i.e., hexagonal ring-shaped radiating patch. The manuscript explains the hexagonal ring-shaped patch antenna, and further, amendments have been made in the patch's geometry and partial ground plane of antenna for improving its performance parameters such as impedance bandwidth, reflection coefficient, number of frequency bands, and gain. The evolution of the proposed antenna design and its results (simulated and measured) have been propounded in detail in the upcoming sections. Similar shaped antennas (Hexagonal Ring) have also been delineated in Table 1 for comprehending the aim behind the design of proposed antenna.

Table 1. Comparison of various hexagonal ring-shaped radiating patch antenna.

Reference	Size of antenna (mm^2)	Resonant frequency bands	Maximum bandwidth (GHz)	Number of frequency bands
[14]	37×62	4.5/7.3	7.74	2
[15]	32×40	1.7/2.4/3.1/4.5/6.0	2.09	4
[16]	30×30	2.1/3.5/6.3/8.5/12.7	4.23	5
[17]	75×75	2.44	—	1
[18]	120×120	2.035	0.152	1
[19]	21×21	5.8	1.18	1
Proposed	24×30	1.5/5.4/7.4/12.0/15.6/20.6	3.69	6

2. PROPOSED ANTENNA DESIGN EVOLUTION

The proposed antenna structure has been premeditated on a low-cost glass epoxy FR4 substrate having dielectric constant (ε_r) 4.4, mass density 19,000 kg/m^3, and loss tangent ($\tan\delta$) 0.02 with overall size of $30 \times 24 \times 1.6\,mm^3$. The structure of designed antenna is fed by a microstrip transmission line of 11.83 mm × 1.6 mm, to generate the 50 Ω port impedance. Evolution steps of different structures of the proposed antenna are delineated in Fig. 1. The process of designing the patch of antenna for every step is illustrated in Fig. 2. Initially, a hexagonal ring structure is designed by subtracting the hexagon of radius 'R_2' from the hexagonal shaped radiating patch. The radius of hexagonal patch is calculated

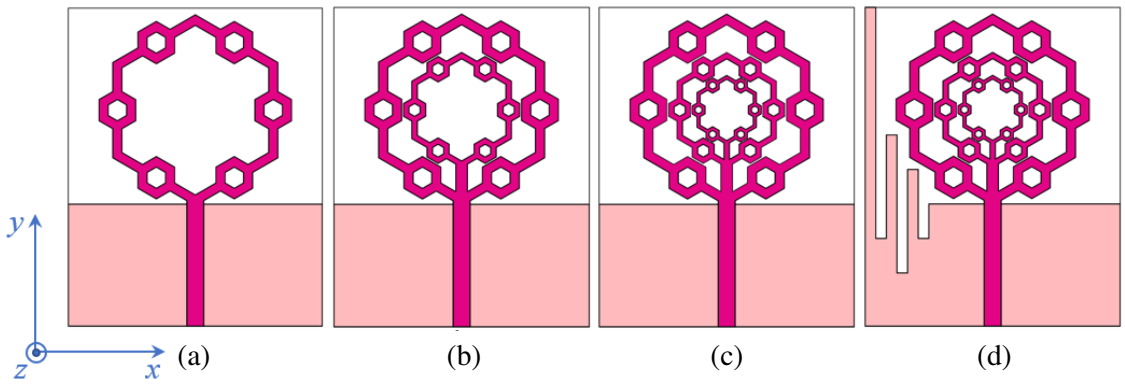

Figure 1. Evolution steps of proposed hexagonal ring-shaped (HRS) fractal antenna: (a) Antenna-1, (b) Antenna-2, (c) Antenna-3 and (d) Antenna-4 (proposed).

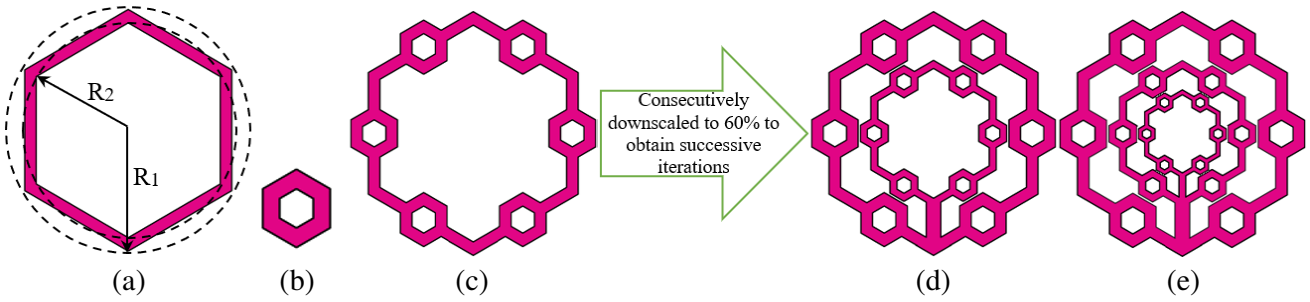

Figure 2. (a) Hexagonal ring, (b) downscaled version of hexagonal ring; HRS fractal patch iterations; (c) 0th iteration, (d) 1st iteration and (e) 2nd iteration (proposed radiating patch).

by using Equations (1)–(2) [20] and found to be 9.0 mm at the designed frequency of 4.43 GHz. This ring structure acts as basic geometry, and further, it is copied and scaled down to 22% of its original size as shown in Fig. 2(b). The smaller ring is then placed repeatedly on the center of each side of bigger hexagonal ring as delineated in Fig. 2(c), also called as the 0th iteration of radiating patch of the proposed antenna.

$$R_1 = \frac{F}{\left\{1 + \frac{2h}{\pi F \varepsilon_r}\left[\ln\left(\frac{\pi F}{2h}\right) + 1.7726\right]\right\}^{\frac{1}{2}}} \tag{1}$$

where,

$$F = \frac{8.791 \times 10^9}{f_r\sqrt{\varepsilon_r}} \tag{2}$$

The final iteration of patch, i.e., the 2nd iteration of HRS radiating patch with modified partial ground plane (loaded with slits and stubs) is illustrated in Fig. 3. The parametric dimensions of all the designed structures are tabulated in Table 2 for better limpidity. The proposed antenna design is compact in the logic of clambering down the lower frequency band of the 0th iterated antenna (Antenna-1 or fractal antenna shown in Fig. 1(a)) from 6.6 GHz to 5.4 GHz with enhanced reflection coefficient of −43.40 dB in Antenna-4 (proposed antenna shown in Fig. 1(d)). With the help of partial ground plane loaded

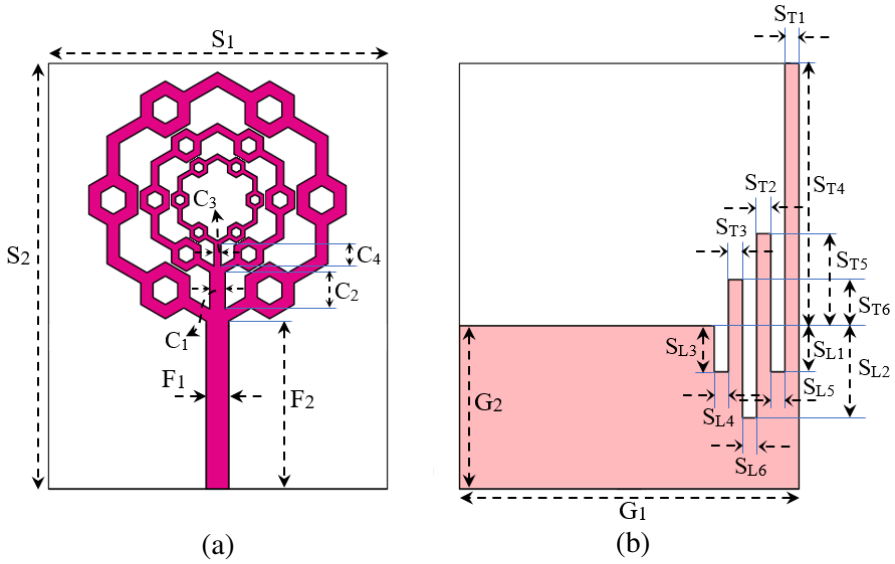

Figure 3. Geometrical structure of proposed HRS fractal antenna; (a) front view and (b) back view.

Table 2. Optimal dimensions of proposed HRS fractal antenna.

Parameter	R_1	R_2	S_1	S_2	C_1	C_2	C_3	C_4	F_1
Dimension (mm)	9.0	8.0	24	30	1.1	2.6	0.5	1.56	1.6
Parameter	F_2	G_1	G_2	S_{T1}	S_{T2}	S_{T3}	S_{T4}	S_{T5}	S_{T6}
Dimension (mm)	11.83	24	11.5	1.0	1.0	1.0	18.5	6.5	3.25
Parameter	S_{L1}	S_{L2}	S_{L3}	S_{L4}	S_{L5}	S_{L6}			
Dimension (mm)	3.25	6.5	3.25	1.0	1.0	1.0			

with slits and stubs, the proposed antenna exhibits an additional frequency band at 1.5 GHz with corresponding reflection coefficient −58.33 dB and impedance bandwidth of 1.88 GHz (96.90%) in the frequency range (1.0 to 2.88 GHz).

The evolution of radiating patch has been started from the design of HRS patch with radii R_1, R_2. For attaining the 0th iterated radiating patch for the generation of Antenna-1, limned in Fig. 1(a), antenna's ring structure has been scaled down, and its corresponding reflection coefficient curve is illustrated in dashed red color line in Fig. 4. The juxtaposition in terms of reflection coefficient of all other successive structures of antennas from Antenna-2 to 4 (proposed antenna) is portrayed in Fig. 4. It can be contemplated from Fig. 4 that Antenna-1, 2, and 3 exhibit five resonant points with a lower band (first frequency band) at 6.6, 7.1, and 7.2 GHz, respectively. In the final step (Antenna-4), the partial ground plane of "Antenna-3" has been modified to generate the additional frequency band at lower side and also to enhance the impedance bandwidth of antenna, as delineated in solid royal blue color line in Fig. 4. The employment of slits and slots in the partial ground plane delivers additional current tracks, thus altering the capacitance and inductance of the antenna system and, in turn, ensuing the exhibition of extra frequency band and improving the impedance bandwidth. The comparisons of various performance parameters of designed antennas (Antenna-1 to Antenna-4) are illustrated in Table 3 for better understanding.

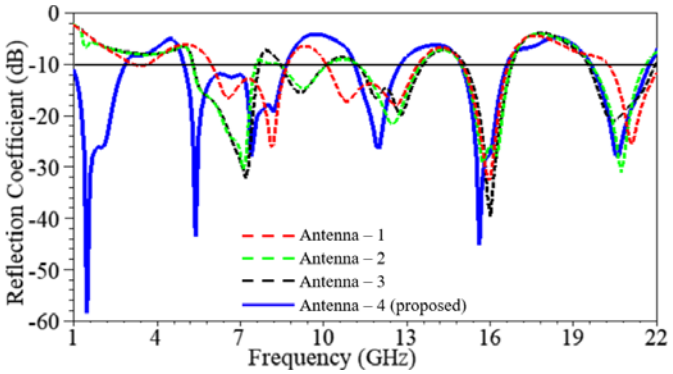

Figure 4. Simulated variation in value of reflection coefficient parameter for Antenna-1 to Antenna-4 (proposed).

The evolution stages for the development of modified ground plane from step-1 to step-5, without making any changes in radiating patch, are projected in Fig. 5. In the first step, the stub (stub-1) of dimensions $S_{T1} \times S_{T4}$ has been united to the upper right-side corner of partial ground plane delineated in Fig. 5(a). Similarly, in the second and third steps, stub-2 and 3 with dimensions $S_{T2} \times S_{T5}$ and $S_{T3} \times S_{T6}$ have been introduced and envisaged in Figs. 5(b) and (c), respectively. Further, in the fourth step, the two slits (slit-1 and 2) with dimensions $S_{L1} \times S_{L5}$ and $S_{L3} \times S_{L4}$ are etched from the geometry obtained in the previous step as shown in Fig. 5(d). Likewise, one more slit called slit-3 with dimension $S_{L2} \times S_{L6}$ has been etched to obtain the final structure of modified ground plane. The frequency responses in terms of reflection coefficient of every stage for the evolution of ground plane are

Table 3. Comparison of results for different structures of designed antenna.

Antenna design	Resonant Frequency (GHz)			Reflection coefficient (dB)	Bandwidth (GHz)	Bandwidth Ratio
	F_L	F_C	F_U			
Antenna-1	5.96	6.6		−16.64	2.74	1.45 : 1
		8.1	8.7	−25.93		
	10.1	12.6	13.4	−18.02	3.30	1.32 : 1
	14.98	15.9	16.65	−32.30	1.67	1.11 : 1
	20.22	21.1	22.00	−25.52	1.78	1.08 : 1
Antenna-2	5.29	7.1	7.57	−30.43	2.28	1.43 : 1
	8.38	9.3	10.18	−14.77	1.80	1.12 : 1
	11.2	12.5	13.5	−21.71	2.30	1.20 : 1
	14.93	15.7	16.75	−29.12	1.82	1.21 : 1
	19.61	20.7	21.58	−30.96	1.97	1.10 : 1
Antenna-3	5.31	7.2	7.69	−32.25	2.38	1.44 : 1
	8.45	9.2	10.10	−15.53	1.65	1.19 : 1
	11.21	12.8	13.60	−19.91	2.39	1.21 : 1
	15.07	16.0	16.78	−39.68	1.71	1.11 : 1
	19.50	20.4	21.93	−21.10	2.43	1.12 : 1
Antenna-4 (proposed)	1.0	1.5	2.88	−58.33	1.88	2.88 : 1
	4.98	5.4		−43.40	3.69	1.74 : 1
		7.4	8.67	−27.97		
	11.11	12.0	12.76	−26.61	1.65	1.14 : 1
	14.94	15.6	16.60	−45.15	1.66	1.66 : 1
	19.61	20.6	21.73	−28.05	2.12	1.10 : 1

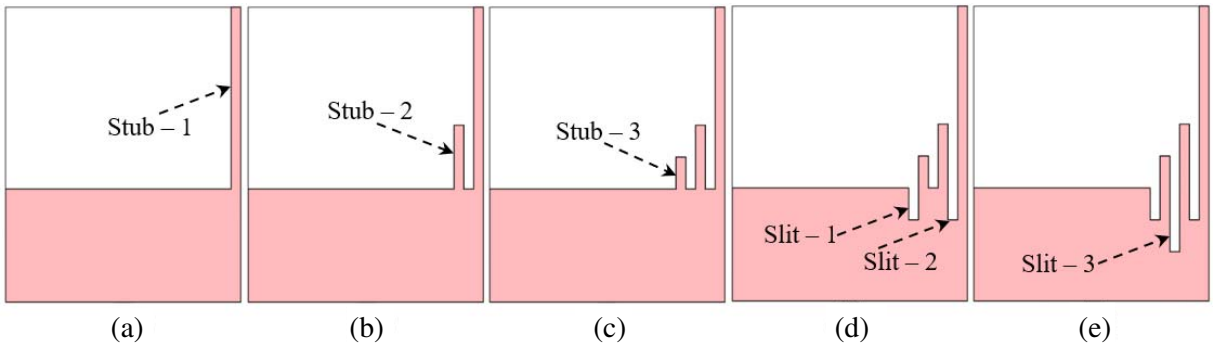

Figure 5. Evolution stages of ground plane: (a) step-1, (b) step-2, (c) step-3, (d) step-4 and (e) step-5.

compared and expounded in Fig. 6. It can be observed from Fig. 6 that by employing stub-1, 2, and 3, consecutively from step-1 to 3, the antenna exhibits the first frequency band at 2.8 GHz with reflection coefficient nearly at −20 dB. The improvement in reflection coefficient and impedance bandwidth of other frequency bands has also been noted in the successive steps of modified ground plane. Further, in the fourth step, slit-1 and 2 have been introduced due to which the initial frequency band is shifted from 2.8 GHz to 2.5 GHz with improved reflection coefficient of −32.82 dB. Finally, in the last step (step-5), slit-3 has been etched from the structure of ground plane obtained in step-4, and the first frequency

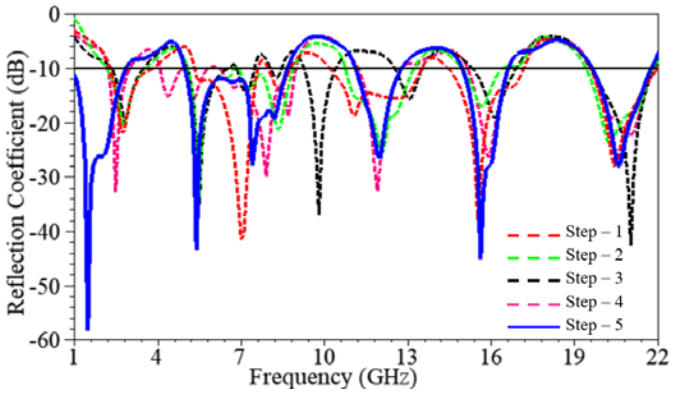

Figure 6. Simulated variation of reflection coefficient response for each evolution stage of modified partial ground plane.

band has been shifted from 2.5 GHz to 1.5 GHz with enhanced reflection coefficient of −58.33 dB and impedance bandwidth of 1.88 GHz (96.90%) in the frequency range from 1.0 to 2.88 GHz. From the above-mentioned discussion, it can be undoubtedly agreed that the modification in partial ground plane of the proposed antenna plays a very important role in achieving the miniaturized form of antenna along with improvement in reflection coefficient and impedance bandwidth.

2.1. Current Distribution and Input Impedance

The surface current distributions of the proposed antenna at distinct frequency bands are plotted and elucidated in Fig. 7. It can be anticipated from Fig. 7(a) that maximum current is concentrated on the modified ground plane (loaded with slits and slots) along with fractal radiating patch and transmission

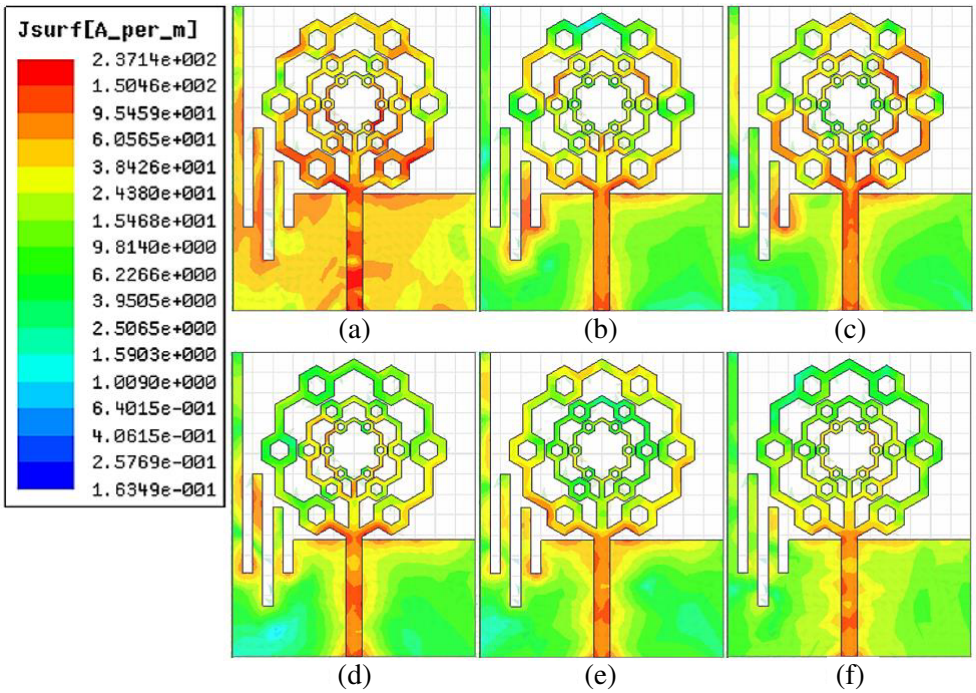

Figure 7. Surface current distribution on the radiating patch and modified ground plane of proposed antenna at; (a) 1.5, (b) 5.4, (c) 7.4, (d) 12.0, (e) 15.6 and (f) 20.6 GHz frequency bands.

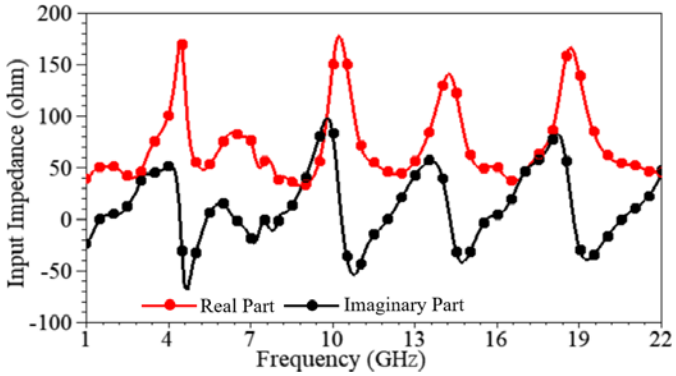

Figure 8. Simulated input impedance variation curves of proposed HRS fractal antenna.

feed line, due to which the antenna exhibits additional frequency band at 1.5 GHz in juxtaposition to the simple partial ground plane loaded antenna. Further, at other frequency bands such as 5.4 and 7.4 GHz, the current is primarily concentrated on radiating patch as well as on stub-3 and slit-1, which helps in the enhancement of impedance bandwidth from 4.98 to 8.67 GHz (3.69 GHz). Finally, as the frequency of antenna increases, the current will get saturated at the slits and slot of the partial ground plane along with transmission line feed which helps to attain the improved reflection coefficient at 12.0, 15.6, and 20.6 GHz frequency bands in comparison to other structures of antenna. Fig. 8 reveals the simulated real and imaginary variation curves of input impedance. It can be observed that real and imaginary parts of impedance have wavered around 50 Ω to 0 Ω for the operating frequency ranges of antenna. Therefore, it can be considered that the resulting input impedance nearly matches the characteristic impedance of the microstrip transmission feed line (50 Ω).

3. FABRICATED PROTOTYPE AND TEST RESULTS

The fabricated prototype of front and rear views of the proposed antenna is shown in Fig. 9. The experimental (measured) and simulated (numerical) reflection coefficient responses have been juxtaposed, reported in Fig. 10, and predicted as a reasonable pact between them. The measurement has been carried out by using calibrated Vector Network Analyzer (VNA). The juxtaposition between the measured and simulated reflection coefficients at distinct operative frequencies has been made and shown in Fig. 10, and found the small variations between them, which may arise due to environmental conditions, parasitical capacitances, inductance at the solder joint of SMA connector, ambiguity in the electrical properties of the material used for designing the antenna, etc. Though above-said ambiguities play a paramount role in the variations of simulated and measured reflection coefficients, yet they have very little impact on impedance bandwidth of antenna. Similarly, modification in the ground plane also indicates insignificant impact on the bandwidth of antenna.

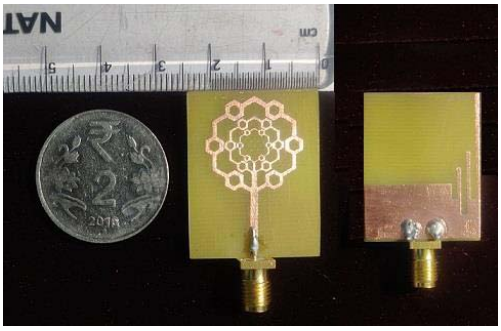

Figure 9. Front and back views of the fabricated prototype of proposed antenna.

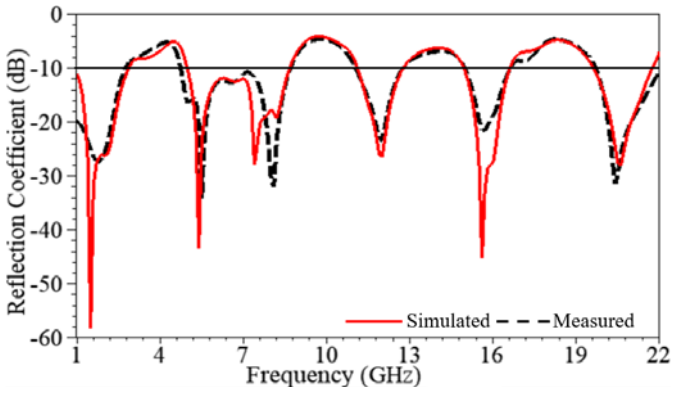

Figure 10. Comparison of simulated and measured reflection coefficient response for proposed HRS fractal antenna.

Figure 10, anticipates that measured proposed antenna reveals six frequency bands with impedance bandwidths of 1.75 GHz (1.0–2.75 GHz), 3.96 (4.74–8.70 GHz), 1.72 GHz (11.04–12.76 GHz), 1.65 GHz (14.97–16.62 GHz), and 2.30 GHz (19.7–22.0 GHz) which are almost equal to the simulated frequency response. From above-said points, the first band covers the 1800 MHz 2G spectrum of GSM band (1.71–1.88 GHz), Aircraft Surveillance (1.09 GHz), 3G Cellular Communication Mobile Uplink (1.90–1.98 GHz), Advance Wireless Services (2.11–2.15 GHz), LTE 2300/LTE 2500 (2.3–2.4 GHz/2.5–2.69 GHz), RFID (2.4 GHz), Wi-Fi (2.4–2.485 GHz), and Bluetooth (2.4 GHz). Similarly, the second and third frequency bands cover the 5G spectrum band (5900–6400 MHz) adopted by European Union, Long Term Evolution (LTE) band 46 (5150–5925 MHz), RFID (5.4 GHz), WLAN (5.15–5.35 and 5.72–5.85 GHz), ISM (5.725–5.875 GHz), Wi-MAX (5.25–5.85 GHz), ITU band (7.8–8.4 GHz), television broadcasting (7.91–8.62 GHz), point-to-point wireless applications (5.925–8.5 GHz), and military band (5.8–7.707 GHz). Likewise, the fourth frequency band used for broadcasting satellites (12.4–12.5 GHz) and FSS (11.45–11.7/12.5–12.75 GHz), whereas the fifth and sixth frequency bands cover the wireless applications like defence systems (14.62–15.23 GHz), aeronautical radio navigations (15.43–17.3 GHz), fixed and mobile satellite communications (19.7–20.1 GHz and 20.2–21.2), earth exploration satellite (21.2–21.4 GHz), and fixed and mobile broadcasting satellite (21.4–22.0 GHz).

The radiation pattern indicates a pictorial representation of the changes in the field strength of the radio waves in 2D/3D space. Usually, 2D radiation patterns are considered at single resonant frequency, single polarization, and single plane cut. Radiation patterns are normally presented in the polar or rectilinear form with dB strength scale because patch antenna radiates normally to its radiating patch surface. Fig. 11 shows the juxtaposition of experimental and simulated radiation patterns at each operating frequency for distinct values of theta. Red line illustrates the value for azimuth angle in E-plane, and royal blue line discerns the value of elevation angle in H-plane. As per the dotted line is concerned, it propounds the measured value of radiation pattern in both the planes. The proposed antenna exhibits nearly omnidirectional patterns in both E- and H-planes at the entire operative bands, which evidently specifies the proposed antenna as a suitable candidate useful for wideband as well as multiband applications. The comparison between simulated and measured peak realized gains versus frequency is drawn and portrayed in Fig. 12 in the desired frequency ranges. This clearly shows that the measured and simulated gain responses are in good agreement with each other. It can also be noted that the antenna's gain varies from 2.83 to 3.37 dB, 0.15 to 2.03 dB, 1.69 to 3.33 dB, 2.75 to 2.98 dB, and 3.03 to 9.98 dB in the achieved operational frequency ranges.

The proposed antenna's characteristics are juxtaposed with existing antennas and delineated in Table 4. Two columns, named "method used" and "remarks" of Table 4, help to understand the comparison of published work with the proposed antenna in a better way. Antennas reported in Table 4 are designed and fabricated on an FR4 glass epoxy substrate with relative permittivity of 4.4. It can be anticipated from the table that the proposed antenna is a compact size antenna in comparison to other existing antennas and also has higher impedance bandwidth as well as a greater number of resonant frequency bands. By scrupulously visualizing the Table and from afore-said discussion, it

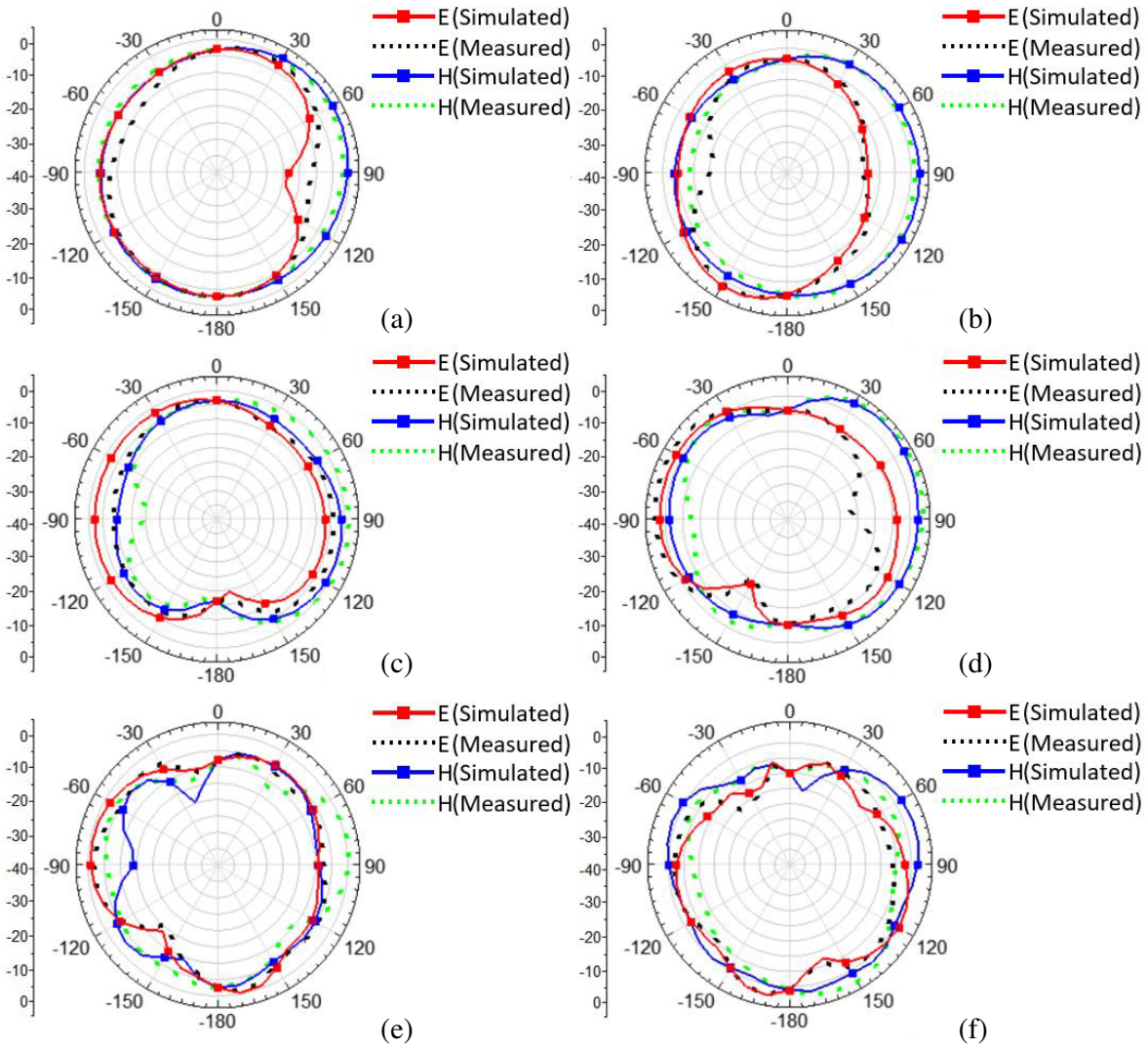

Figure 11. Simulated and measured radiation pattern of proposed HRS fractal antenna in E and H-plane at; (a) 1.5, (b) 5.4, (c) 7.4, (d) 12.0, (e) 15.6 and (f) 20.6 GHz frequency bands.

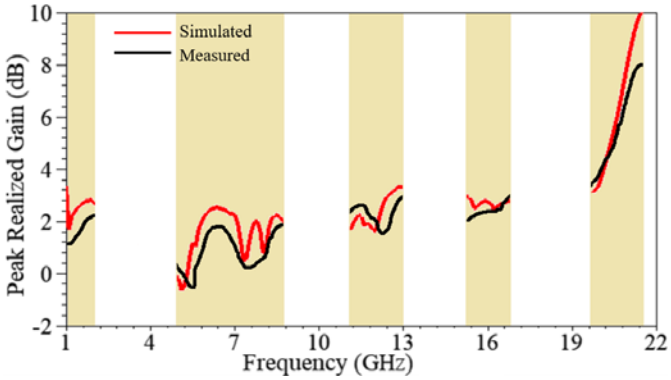

Figure 12. Comparison of simulated and measured peak realized gain response for proposed HRS fractal antenna.

Table 4. Comparison of proposed hexagonal ring-shaped antenna with other existing published works.

Reference	Size (mm^2)	Bandwidth (GHz)	Gain (dB)	Method used	Remarks/Comments
[21]	58×40	1.51–3.69 4.67–5.25 5.78–5.96	5.2 4.85	Wheel shaped fractal radiating patch with defected ground plane	Less compact
[22]	40×40	3.86–3.94 5.96–7.38 8.2–8.9	0.1–0.2 1.9–2.8 0.1–2.8	H-tree shaped fractal antenna using CPW fed	Not covered lower frequency band; exhibit less gain; less compact
[23]	44.6×51.5	4.82–6.26	7.73	U-shaped slot loaded rectangular patch with U parasitic elements	Less compact in size and not covered lower frequency band
[24]	44.92×45	3.0–5.48	5.1	Meander fractal element loaded hexagonal patch antenna	Less compact in size and not covered lower frequency band
[25]	54.4×35.6	4.56–7.92	Not Given	Plus-shaped fractal radiating patch with CPW fed	Less compact in size and not covered lower frequency band
[26]	42×23	4.72–5.95	2.0–6.0	Parasitic patch with ring-shaped radiator	Not covered lower frequency band
[27]	34×51	4.8–5.1 5.8–6.8	2.3 4.7	Defected ground plane loaded Fibonacci word fractal	Exhibit less gain; Less compact in size and not covered lower frequency band
[28]	34×51	1.65–2.59 4.16–4.52 5.54–6.42	1.7 1.6 2.3	Circular radiating patch loaded with hexagonal slot	Less compact in size with low gain
[29]	48×48	3.95–4.05 5.82–5.98	0.8 7.4	Hybrid geometry of Sierpinski and Minkowski fractal curves	Less compact in size and not covered lower frequency band
[30]	27×50	1.63–1.88 4.5–8.5	1.97 5.05	Plus-shaped fractal radiating patch with defected ground structure	Not covered lower frequency band; low gain; less compact
Proposed	24×30	1.0–2.88 4.98–8.87 11.11–12.76 14.94–16.60 19.61–21.73	2.83–3.37 0.15–2.03 1.69–3.33 2.75–2.98 3.03–9.98	Defected ground plane loaded hexagonal ring-shaped fractal radiating patch antenna with hexagonal ring elements	Exhibit high gain; more compact in size and also covers the lower frequency band of operation

can be advocated that proposed antenna particularizes hexa frequency bands with wider bandwidth and improved gain at each frequency resonance point in juxtaposition to the antennas discussed in References [21–30].

4. CONCLUSION

A hexagonal ring-shaped fractal antenna with stubs and slits loaded partial ground plane has been expounded for hexa-band operations with stable radiation pattern and gain. The proposed antenna is economical, compact sized, and exhibits impedance bandwidth ($S_{11} \leq -10\,\text{dB}$) in the frequency ranges 1.0–2.75 GHz, 4.74–8.70 GHz, 11.04–12.76 GHz, 14.97–16.62 GHz, and 19.70–22.0 GHz, and covers distinct wireless standards. The peak realized gain of proposed antenna varies from 2.83 to 3.37 dB, 0.15 to 2.03 dB, 1.69 to 3.33 dB, 2.75 to 2.98 dB, and 3.03 to 9.98 dB in the operational frequency ranges. The proposed antenna also reveals almost omnidirectional radiation patterns in E- and H-planes at all resonant frequency bands. Characteristics of the proposed antenna have also been compared with existing similar kinds of published work in Table 4, and it is compact in size and reports better performance than the other antennas.

REFERENCES

1. Mandelbrot, B.-B., *The Fractal Geometry of Nature*, San Francisco, W.H. Freeman and Company, California, 1982.
2. Sharma, N. and V. Sharma, "A journey of antenna from dipole to fractal: A review," *J. Eng. Technol.*, Vol. 6, No. 2, 317–351, 2017.
3. Sharma, N. and S.-S. Bhatia, "Double split Labyrinth resonator based CPW-fed hybrid fractal antennas for PCS/UMTS/WLAN/Wi-MAX applications," *Journal of Electromagnetic Waves and Applications*, Vol. 33, No. 18, 2476–2498, 2019.
4. Sharma, N., V. Sharma, and S. S. Bhatia, "A novel hybrid fractal antenna for wireless applications," *Progress In Electromagnetics Research M*, Vol. 73, 25–35, 2018.
5. Sharma, N. and V. Sharma, "A design of microstrip patch antenna using hybrid fractal slot for wideband applications," *Ain. Shams. Eng. J.*, Vol. 9, No. 4, 2491–2497, 2018.
6. Kaur, M., and J.-S. Sivia, "Minkowski, Giuseppe Peano and Koch curves-based design of compact hybrid fractal antenna for biomedical applications using ANN and PSO," *AEU-Int. J. Electon. and Commun.*, Vol. 99, 14–24, 2019.
7. Bangi, I.-S. and J.-S. Sivia, "Moore, Minkowski and Koch curves-based hybrid fractal antenna for multiband applications," *Wireless Pers. Commun.*, Vol. 108, 2435–2448, 2019.
8. Kumar, Y. and S. Sing, "A compact multiband hybrid fractal antenna for multi-standard mobile wireless applications," *Wireless Pers. Commun.*, Vol. 84, 57–67, 2015.
9. Shahu, B.-L., N. Chattoraj, S. Pal, and D.-K. Upadhyay, "A compact UWB bandpass filter using hybrid fractal shaped DGS," *J. Microw., Optoelect. and Electromag. App.*, Vol. 16, No. 1, 38–49, 2017.
10. Choukiker, Y.-K., S.-K. Sharma, and S.-K. Behera, "Hybrid fractal shape planar monopole antenna covering multiband wireless communications with MIMO implementation for handheld mobile devices," *IEEE Trans. on Ant. and Propag.*, Vol. 62, No. 3, 1483–1488, 2014.
11. Sharma, N., S. Kaur, and B.-S. Dhaliwal, "A new triple band hybrid fractal boundary antenna," *IEEE Int. Conf. Recent Trends Electron., Info. & Commun. Technol.*, 2016, doi: 10.1109/RTEICT.2016.7807953.
12. Bangi, I.-S. and J.-S. Sivia, "A compact hybrid fractal antenna using Koch and Minkowski curves," *IEEE 9th Annual Info. Technol., Electron. and Mobile Commun. Conf.*, 2018, doi: 10.1109/IEMCON.2018.8614773.
13. Goyal, N., S. Singh, and A. Marwaha, "Hybrid fractal microstrip patch antenna for wireless applications," *Int. Conf. Next Gen. Comput. Technol.*, 2015, doi: 10.1109/NGCT.2015.7375160.
14. Kaur, N., J. Singh, and M. Kumar, "Hexagonal ring-shaped dual band antenna using staircase fractal geometry for wireless applications," *Wireless Pers. Commun.*, Vol. 113, 2067–2078, 2020.
15. Mark, R., N. Mishra, K. Mandal, P.-P. Sarkar, and S. Das, "Hexagonal ring fractal antenna with dumb bell-shaped defected ground structure for multiband wireless applications," *AEU-Int. J. Electon. and Commun.*, Vol. 94, 42–50, 2018.
16. Sharma, N. and S.-S. Bhatia, "Performance enhancement of nested hexagonal ring-shaped compact multiband integrated wideband fractal antennas for wireless applications," *Int. J. RF Microw. Aided. Eng.*, Vol. 30, No. 3, 1–21, 2019.
17. Rathod, S.-M., P. Jadhav, R.-N. Awale, K.-P. Ray, and S.-S. Kakatkar, "Low profile hexagonal ring patch antenna for biomedical application," *Int. Conf. Comput. Commun. Cont. Autom.*, 2017, doi: 10.1109/ICCUBEA.2016.7860089.
18. Ray, K.-P., S.-S. Kakatkar, S.-M. Rathod, R.-N. Awale, and D.-P. Rathod, "Investigation of hexagonal ring microstrip antenna," *Int. Conf. on Microw., Optic and Commun. Eng.*, 2015, doi: 10.1109/ICMOCE.2015.7489717.
19. Daniel, R. S. and R. Selvaraj, "A low-profile split ring monopole antenna loaded with hexagonal split ring resonator for RFID applications," *Progress In Electromagnetics Research M*, Vol. 92, 169–179, 2020.

20. Bhatia, S. S. and N. Sharma, "A compact wideband antenna using partial ground plane with truncated corners, L-shaped stubs and inverted T-shaped slots," *Progress In Electromagnetics Research M*, Vol. 97, 133–141, 2020.
21. Madhav, B. T. P. and A. Tirunagari, "Design and study of multiband planar wheel-like fractal antenna for vehicular communication applications," *Microw. Optic. Technol. Lett.*, Vol. 60, 1985–1993, 2018.
22. Reha, A., A. El Amri, O. Benhmammouch, A. O. Said, A. El Ouadih, and M. Bouchouirbat, "CPW-fed H-tree fractal antenna for WLAN, WIMAX, RFID, C-band, HiperLAN, and UWB applications," *Int. J. Microw. Wirel. Technol.*, Vol. 8, 327–334, 2016.
23. Lu, H.-X., F. Liu, S. Ming, and Y.-A. Liu, "Design and analysis of wideband U-slot patch antenna with U-shaped parasitic elements," *Int. J. RF Microw. Comput. Aided Eng.*, Vol. 28, No. 2, e21202, 2018.
24. Bhatia, S. S., J. S. Sivia, and N. Sharma, "An optimal design of fractal antenna with modified ground structure for wideband applications," *Wirel. Pers. Commun.*, Vol. 103, 1977–1991, 2018.
25. Kakkar, S. and S. Rani, "Implementation of fractal geometry to enhance the bandwidth of CPW fed printed monopole antenna," *IETE J. Res.*, Vol. 63, 23–30, 2017.
26. Deng, C., "Wideband microstrip antennas loaded by ring resonators," *IEEE Antennas Wirel. Propag. Lett.*, Vol. 12, 1665–1668, 2013.
27. Singh, G. and A. P. Singh, "On the design of planar antenna using Fibonacci word fractal geometry in support of public safety," *Int. J. RF Microw. Comput. Aided Eng.*, Vol. 29, No. 2, e21554, 2019.
28. Joseph, S., B. Paul, S. Mridula, and P. Mohanan, "A novel planar fractal antenna with CPW-feed for multiband applications," *Radioeng. J.*, Vol. 22, 1262–1266, 2013.
29. Vallappil, A. K., B. A. Khawaja, I. Khan, and M. Mustaqim, "Dual-band Minkowski-Sierpinski fractal antenna for next generation satellite communications and wireless body area networks," *Microw. Optic. Technol. Lett.*, Vol. 60, 171–178, 2018.
30. Puri, S.-C., S. Das, and M.-G. Tiary, "A multiband antenna using plus-shaped fractal-like elements and stepped ground plane," *Int. J. RF Microw. Comput. Aided Eng.*, Vol. 30, No. 5, e22169, 2020.